Oncogene (2016) **35,** 4981–4989

www.nature.com/onc

ORIGINAL ARTICLE

The Δ133p53 isoform and its mouse analogue Δ122p53 promote invasion and metastasis involving pro-inflammatory molecules interleukin-6 and CCL2

I Roth[1,2,6], H Campbell[3,6], C Rubio[3], C Vennin[4], M Wilson[1], A Wiles[1], G Williams[1], A Woolley[1], P Timpson[4], MV Berridge[5], N Fleming[1], M Baird[1,2] and AW Braithwaite[1,2,3]

A number of naturally occurring isoforms of the tumour suppressor protein p53 have been discovered, which appear to have differing roles in tumour prevention or promotion. We are investigating the tumour-promoting activities of the Δ133p53 isoform using our mouse model of Δ133p53 (Δ122p53). Here, we report that tumours from Δ122p53 homozygous mice show evidence of invasion and metastasis and that Δ122p53 promotes migration though a 3-dimensional collagen matrix. We also show that Δ122p53 and Δ133p53 promote cell migration in scratch wound and Transwell assays, similar to the 'gain-of-function' phenotypes seen with mutant p53. Using the well-defined B16 mouse melanoma metastatic model, we show that Δ122p53 leads to faster generation of lung metastases. The increased migratory phenotypes are dependent on secreted factors, including the cytokine interleukin-6 and the chemokine CCL2. We propose that Δ122p53 (and Δ133p53) acts in a similar manner to 'gain-of-function' mutant p53 proteins to promote migration, invasion and metastasis, which may contribute to poor survival in patients with Δ133p53-expressing tumours.

Oncogene (2016) **35,** 4981–4989; doi:10.1038/onc.2016.45; published online 21 March 2016

INTRODUCTION

TP53 is the canonical tumour suppressor gene that is essential for cancer prevention. Wild-type (wt) p53 prevents tumour development by several mechanisms, including cell cycle arrest and apoptosis of damaged cells, thus preventing the expansion of mutant and therefore potentially tumorigenic cell clones. Wt p53 may also prevent tumour development by preventing migration and angiogenesis, two important processes in the development of a metastatic tumour. Wt p53 is thought to prevent migration through a suppressive mechanism, as p53-deficient mouse embryonic fibroblasts (MEFs) have increased migratory ability in scratch wound assays.[1–5] Wt p53 also prevents angiogenesis by maintaining the angiogenic balance via regulating factors such as the pro-angiogenic factor HIF-1α,[6] and the anti-angiogenic thrombospondin-1 (TSP-1).[7,8] In combination, wt p53 also acts to prevent tumour cell migration, invasion and metastasis.

In addition to full-length (FL) p53 protein, the *TP53* gene also encodes at least 13 isoforms that appear to have differing functions. These can be sub-grouped according to where the proteins start within the *TP53* gene. The Δ40p53 isoforms are lacking the first 39 N-terminal amino acids and are generated by alternative splicing of exon 2 and the use of the alternative start codon at residue 40. There is also alternative C-terminal splicing of exons 9 and 10 to generate Δ40p53α, β and γ isoforms. Similarly, the Δ133p53 family is lacking the first 132 amino acids. It is generated from transcripts initiated from a promoter in intron 4 and has the same C-terminal splicing as the Δ40p53 family, also generating three isoforms. In addition, an alternative start codon is used to generate the Δ160p53 isoforms, and finally, the FL p53 can also vary at the C-terminus in the same manner (reviewed by Marcel *et al.*[9]). Recently, a further isoform was reported, p53Ψ, which results from the use of an alternative splice acceptor site at the 3′ end of intron 6.[10]

Several of these p53 isoforms are aberrantly expressed in human cancer cell lines and human cancers. For example, the Δ133p53 isoform is aberrantly expressed in breast cancer,[11] head and neck cancer,[12] melanoma,[13] renal cell[14] and colon carcinomas.[15] Elevated expression of Δ133p53 expression has also been shown to be associated with poor prognosis in cholangiocarcinoma.[16] Consistent with a role in cancer progression, Δ133p53 was found to promote invasion and angiogenesis of U87 glioblastoma cells.[17] These data suggest that Δ133p53 might be involved in promoting invasion and metastasis.

Although the isoforms appear to be dysregulated in tumours, their exact role in tumorigenesis is unclear. Some of the isoforms have been shown to enhance p53 activity, such as p53β, which has been shown to cooperate with FLp53 on some promoters, including the *BAX* promoter.[18] Others have been shown to repress the canonical functions of FLp53, whereas some studies have suggested that some of the p53 isoforms may have functions independent of FLp53. Both Δ40p53 and Δ133p53 have also been shown to enhance FLp53 when expressed at low levels, but inhibit the canonical functions of p53 when expressed at higher levels,[18,19] indicating that these isoforms may form an intricate control network for the p53 family.

[1]Department of Pathology, Dunedin School of Medicine, University of Otago, Dunedin, New Zealand; [2]Maurice Wilkins Centre for Molecular Biodiscovery, School of Biological Sciences, University of Auckland, Auckland, New Zealand; [3]Children's Medical Research Institute, University of Sydney, Sydney, New South Wales, Australia; [4]The Garvan Institute of Medical Research, Sydney, New South Wales, Australia and [5]Malaghan Institute for Medical Research, Wellington, New Zealand. Correspondence: Professor AW Braithwaite, Department of Pathology, Dunedin School of Medicine, University of Otago, 58 Hanover Street, Dunedin, New Zealand.
E-mail: antony.braithwaite@otago.ac.nz
[6]These authors contributed equally to this work.
Received 16 September 2015; revised 17 December 2016; accepted 8 February 2016; published online 21 March 2016

Previously, we reported studies with a mouse expressing an N-terminally truncated p53 mutant, Δ122p53, which is similar to the human Δ133p53 isoform.[20] These studies showed that the Δ122p53 mutant could function as an oncogene with mice displaying a complex tumour spectrum with aggressive T- and B-cell lymphomas and sarcomas.[20] In addition, Δ122p53 mice had a distinct pro-inflammatory phenotype, including elevation of several pro-inflammatory cytokines and chemokines.[20]

To further explore the mechanism of the oncogenic function of Δ122p53, we investigated whether Δ122p53 promotes a migratory and invasive phenotype. Here, we show that both Δ133p53 and Δ122p53 promote migration in scratch wound, Transwell and 3-dimensional (3D) organotypic assays. We also show that Δ122p53 promotes invasion and metastasis of B16 melanoma cells to the lungs of recipient mice. Finally, we show that this migration and invasion requires secretion of interleukin-6 (IL-6) and CCL2, factors also found in the senescence-associated secretory phenotype. We propose that Δ122p53 (and by inference Δ133p53) increases serum levels of these factors to promote tumour migration and invasion, which may in part be responsible for the poor prognosis of patients with tumours displaying elevated levels of Δ133p53.

RESULTS

Δ122p53 mice readily develop metastatic tumours

To address whether Δ122p53 promotes the development of invasive and metastatic tumours, histopathology analysis was carried out on tissues derived from a small cohort of animals with a Δ122p53 allele (Δ122p53/+ or Δ122p53/Δ122p53). We found that metastatic sarcomas were present in 10/14 mice, which is distinct from p53-null mice, which, while developing sarcomas, none were metastatic. An example of a primary sarcoma is shown in Figure 1a, with the primary tumour evident in the submucosa of the colon. Metastases to the liver, pancreas and spleen are also shown (Figures 1b–d, respectively). These results suggest that Δ122p53 increases tumour aggression and promotes metastasis.

Overexpression of the Δ133p53 isoform promotes migration and a loss of persistence

To test whether Δ133p53 promotes migration, the p53-null Saos-2 osteosarcoma cell line was stably transduced with either a Δ133p53 expression construct (Saos/Δ133) or control vector (Saos/vector) (see Materials and methods for construction and Supplementary Figure 1A for western blot showing expression) and the scratch wound closure monitored (Supplementary Figure 1B showing image masks of migrating cells, see also Supplementary material online for Supplementary videos 1 and 2 of scratch wound closure) and the times to complete closure quantitated (Figure 2a). Saos/Δ133 cells reduced the scratch wound closure time from an average of 96 h for Saos/vector to 83 h (Figure 2a). Single transduced cells were tracked and the average speed compared. Saos/Δ133 cells had an average speed of 0.05 μM/s while the vector cells had an average speed of 0.023 μM/s (Figure 2b). Next 'persistence' of migration was measured. Persistence is a ratio of the direct distance a cell travels from the starting point until the end point, compared with the actual distance travelled. Mutant p53 cells tend to have poorer persistence or less structured migration.[21] The results show that Saos/Δ133 cells had a poorer persistence than Saos/vector cells, with a ratio of 0.66 versus 0.85 (Figure 2c). Thus, Δ133p53 interrupts the directional persistence of cells, leading to more random cell movement. Using phalloidin to stain the actin filaments of the transduced Saos-2 cells, we show that the Saos/vector cells were largely non-migratory as evidenced by the stellate configuration of the F-actin at the early stages of wound closure (Figure 2e), while the Saos/Δ133 cells showed clear elongation of the actin filaments towards the leading edge of migration (Figure 2f).

Having shown that Δ133p53 promotes migration in the context of scratch wound assays, we next tested whether it could also promote invasion using Transwell inserts coated with Matrigel to act as a model of the extracellular matrix. Cells were serum-starved and then allowed to invade towards the bottom well which contained 10% fetal calf serum. We found that 25–35% more Saos/Δ133 cells invaded through the Matrigel than the Saos/vector controls after 40 h (Figure 2d).

Taken together, these experiments show that overexpression of Δ133p53 promotes migration in scratch wound and Transwell assays, results in a loss of persistence and promotes invasion in an anchorage-independent manner. These properties are similar to the properties of 'gain-of-function' tumour mutants of p53.[22]

Overexpression of the Δ122p53 mutant promotes migration

To determine whether Δ122p53 promotes a migratory phenotype similar to Δ133p53, we performed a similar set of experiments using the mouse p53-null fibroblast cell line 10.1 either transduced with a retrovirus expressing Δ122p53 (10.1/Δ122) or control vector (10.1 /vector) (see Materials and methods for construction and Supplementary Figure 1C for western blot showing expression). In a scratch wound assay, 10.1/Δ122 cells closed more rapidly than 10.1/vector cells, with an average time to close of 16 h compared with 22 h (Figure 3a, representative wound mask images showing scratch wound closure over time are shown in Supplementary Figure 1D, see also Supplementary material online for Supplementary videos 3 and 4 of scratch wound closure). As was observed for Δ133p53, we found that the expression of Δ122p53 increased the average speed of individual cells in a scratch wound assay (0.027 μM/s compared with 0.019 μM/s for the 10.1/vector cells, Figure 3b). We also measured the scratch wound closure time of MEFs derived from p53-null mice, Δ122p53 mice and heterozygous Δ122p53/+ mice. Results (Figure 3c) show that homozygous Δ122p53 MEFs did not close at a rate that was significantly different to p53-null MEFs, however, Δ122p53/+ MEFs closed the scratch wound faster than p53+/− MEFs, with an average time to close of 15 h compared with 20 h, suggesting that the presence of one p53 allele aids Δ122p53 in scratch wound closure.

Using phalloidin to label the actin filaments of the transduced 10.1 cells during a scratch wound assay, we show that the 10.1/vector cells, although polarised at the leading edge, were largely stellate as a population (Figure 3d), while the 10.1/Δ122 population of cells showed a clear polarisation of actin filaments, with extensive elongation towards the leading edge of migration. Interestingly, this was not limited to those cells on the edge of the wound but was also seen in cells further away from the wound (Figure 3e).

Finally, in a Transwell assay, we found that on average twofold more 10.1/Δ122 cells migrate compared with 10.1/vector cells (Figure 4b, examples of images in Figure 4a).

To exclude the possibility that the migratory effects of Δ122p53 are dependent on the ability of Δ122p53 to promote proliferation as previously described,[20] 10.1/Δ122 cells were treated with the topoisomerase inhibitor amsacrine[23] at a concentration sufficient to inhibit proliferation (Supplementary Figure 2A) and a scratch wound assay was carried out. We found that the addition of amsacrine had no significant effect on the scratch wound closure time of these cells (Supplementary Figure 2B). Similar results were observed with 10.1/vector cells (data not shown). Thus, migration of 10.1/Δ122 cells is independent of cell proliferation. This conclusion is supported by the single cell tracking experiments (Figures 2b and c), and Transwell experiments that occur over a 4 h period. Collectively, these data allow us to conclude that Δ122p53, along with Δ133p53, has strong pro-migratory properties, similar to those seen with gain-of-function p53 tumour mutants.

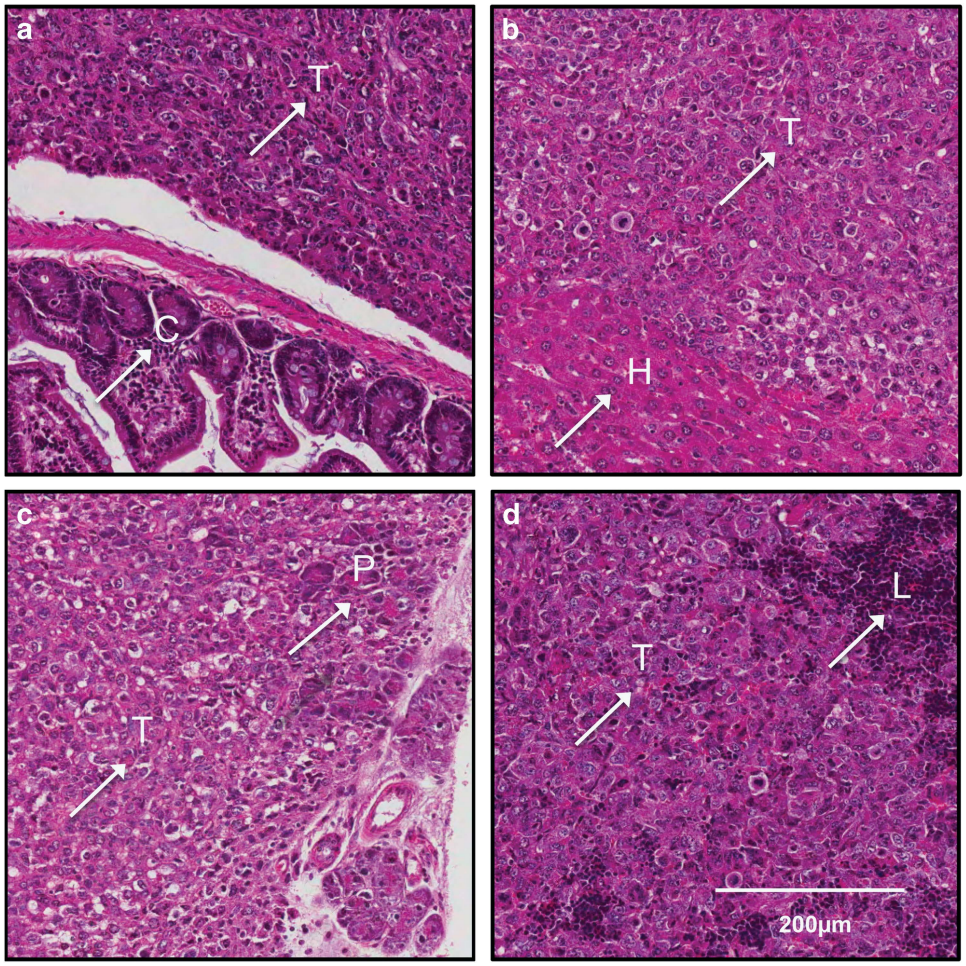

Figure 1. Evidence that Δ122p53 mice develop metastatic tumours. Δ122p53/+ and Δ122p53 homozygous mice were examined histologically for evidence of tumour invasion and metastasis. (**a**) Example of a primary tumour (T) in the submucosa of the colon, with normal colon tissue still evident (C). (**b**) Metastasis to the liver, with tumour (T) evident among remaining hepatocytes (H). (**c**) Metastasis to the pancreas, with pancreatic cells (P) and tumour (T). (**d**) Metastasis to the spleen, with some lymphocytes (L) evident among tumour (T).

Δ122p53 promotes invasion through a 3-dimensional extracellular matrix

To determine whether Δ122p53 can induce invasion in a complex 3-dimensional matrix that mimics *in vivo* conditions, organotypic rafts derived from telomerase-immortalised fibroblasts were used. Briefly, collagen plugs were generated from these cells and mouse pancreatic ductal adenocarcinoma cells (PDAC)[24] transduced with either a vector (PDAC/vector) or Δ122p53 (PDAC/Δ122) were seeded on top. Fourteen days later, the organotypic cultures were harvested and stained to determine invasion of the PDAC cells. Results (Figure 5b) show that PDAC cells transduced with Δ122p53 had a higher invasive index (~50%) compared with the vector control cells (~25%) (see Figure 5a and Supplementary Figure 3 for images of invading cells). Collagen plugs were also generated from Δ122p53/+ MEFs and PDAC/vector and PDAC/Δ122 cells seeded on top. Results again show that ~50% of PDAC/Δ122 cells were invasive compared with ~20% of PDAC/vector cells (data not shown). We also noted that during the contraction of the collagen plugs, Δ122p53/+ MEFs produced looser plugs with less contraction than p53+/+ MEFs (Supplementary Figure 4). This indicates that in addition to positive effects on cell migration, Δ122p53 also has an effect on the extracellular matrix.

Δ122p53 promotes lung metastasis of B16 melanoma cells

As for Saos-2 and 10.1 cells, B16F1 mouse melanoma cells were similarly constructed by transduction with the vector control (B16/vector) or Δ122p53 (B16/Δ122) (see Materials and methods). In Transwell assays, threefold more B16/Δ122 cells migrated than B16/vector cells in the time frame assessed (Figure 4d, with a representative field shown in Figure 4c).

To test whether Δ122p53 can directly promote tissue invasion and metastasis as would be predicted from previous results, we used the well-established B16 melanoma metastasis model.[25] In brief, cells were injected into the tail vein of mice, which rapidly migrate to the lungs where tumour colonies develop over a 21-day period. We found that at day 10, animals receiving B16/Δ122 cells trended towards an increase in numbers of visible melanoma colonies on the lung surface compared with B16/vector animals (Figure 6a). At day 14 and 18, we found no difference in the numbers of visible tumour colonies between B16/vector and B16/Δ122 groups (Figure 6a, see Figure 6b for examples of lungs with tumour colonies at day 14). To further examine our findings, lungs were serially sectioned and tumour size measured throughout the lung. We show that at day 10, Δ122p53 appears to promote rapid tumour growth and development, while by day 18 the tumour area between animals is similar (Figure 6c). Lymphocyte infiltration was seen in both groups at day ten (data not shown), and day 18 (Supplementary Figure 6), however tumour cell invasion into the associated adipose tissue was more extensive in animals receiving B16/Δ122 cells (Figure 6d).

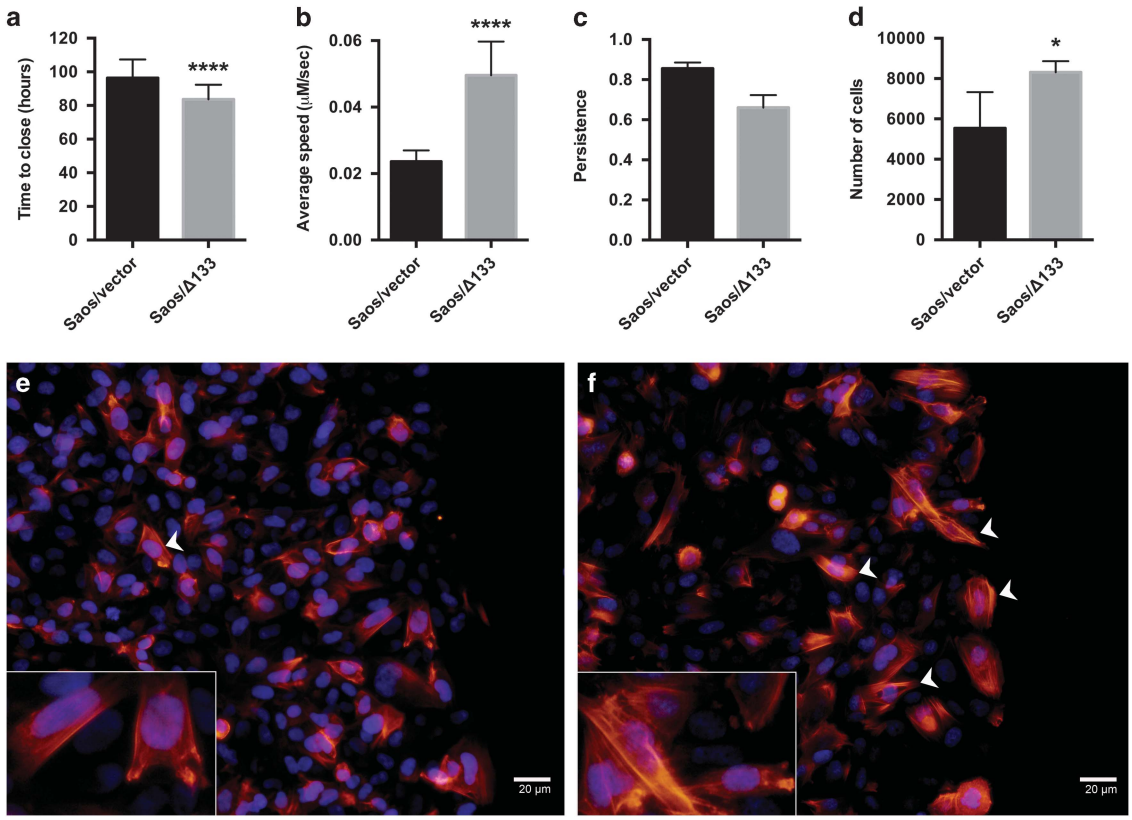

Figure 2. Overexpression of the Δ133p53 isoform promotes scratch wound closure, migration and loss of persistence. Saos/vector and Saos/Δ133 cells were seeded into 96-well plates, and 35-mm dishes, a scratch introduced into the monolayer and closure monitored by time-lapse microscopy. (**a**) Time taken for cells to complete scratch wound closure. (**b**) Individual cells were tracked over time and the average speed of migration determined. (**c**) The path travelled by individual cells was also analysed, and is represented here as persistence. (**d**) Quantitation of invasiveness of Saos/vector and Saos/Δ133 cells in a Transwell assay. (**e**) Immunofluorescence staining of Saos/vector cells stained with phallodin (red) to label actin filaments and Hoechst (blue) to label DNA. Arrow heads indicate cells of interest. (**f**) Immunofluorescence staining of Saos/Δ133 cells stained with phallodin (red) to label actin filaments and Hoechst (blue) to label DNA. Arrow heads indicate cells of interest.

Taken together, these data show that Δ122p53 alters the kinetics of metastasis development in a melanoma model, and further supports that Δ122p53 is an oncogene and has an aggressive pro-metastatic nature.

Cells expressing Δ122p53 secrete factors that promote cell migration

To test whether the increased migration seen in cells expressing Δ122p53 was due to the presence of soluble factors, conditioned media (CM) from MEF cells of indicated genotypes (Figure 7a) was collected after 3–4 days in culture. A scratch wound was introduced into a confluent monolayer of p53+/− MEFs, which was then incubated in the CM and closure times measured. CM from Δ122p53/+ cells decreased closure time of p53+/− MEFs compared with CM from p53+/− cells, with an average time to closure of 19 h compared with 45 h (Figure 7a). We also found that CM from homozygous Δ122p53 cells decreased closure times of p53+/− compared with p53−/− CM, with an average time to closure of 30 h compared with 37 h (Figure 7a). In addition, using p53+/+ MEFs, we found that the addition of CM from Δ122p53/+ cells decreased scratch wound closure time compared with CM from p53+/− cells, with an average time to closure of 28 h compared with 40 h (Supplementary Figure 5A). Thus, we conclude that the pro-migratory phenotype of Δ122p53 is dependent on one or more secreted factors.

To identify the factors that may be responsible for the increased migratory phenotype of cells expressing Δ122p53, we screened CM from Δ122p53/+ cells and compared it with CM from p53+/− cells, using a multiplex suspension array panel (Bio-Plex) containing 23 cytokines and chemokines. Results (Supplementary Figure 5B) show an example of five cytokines/chemokines that were screened, four of which were consistently higher in the CM from Δ122p53/+ cells. These included IL-6, CCL2 (MCP-1), CCL3 (MIP-1α) and CCL4 (MIP-1β), factors that are also common within the senescence-associated secretory phenotype.[26] These are all pro-inflammatory signalling molecules, and during infections, these chemokines act to guide immune cells to the site of infection. CCL2 is a recruiter of monocytes, memory T cells and dendritic cells,[27] while CCL3 mediates endotoxin-induced inflammatory effects,[28] and CCL4 recruits natural killer cells and monocytes,[29] while IL-6 is a pro-inflammatory cytokine that appears to have a role in tumour metastasis.[30] Therefore, all these factors may have a role in the pro-migratory and tumorigenic phenotype we see with Δ122p53 expression.

To determine which identified factor or factors are important in promoting migration of Δ122p53-expressing cells, a Transwell assay was performed using 10.1/Δ122 and 10.1/vector cells as described previously, with the addition of blocking antibodies to the identified candidate factors. We found that the addition of blocking antibodies to IL-6 and CCL2 reduced the number of 10.1/Δ122 cells that were able to migrate across the Transwell (Figures 7b and c, respectively). However, the same was not true of 10.1/vector cells. There was no effect of an isotype control antibody. We observed no effect with the addition of blocking antibodies to CCL4 and CCL5 (data not shown).

To confirm the importance of IL-6 as a contributor to the migratory phenotype, MEFs were used from Δ122p53/+ mice

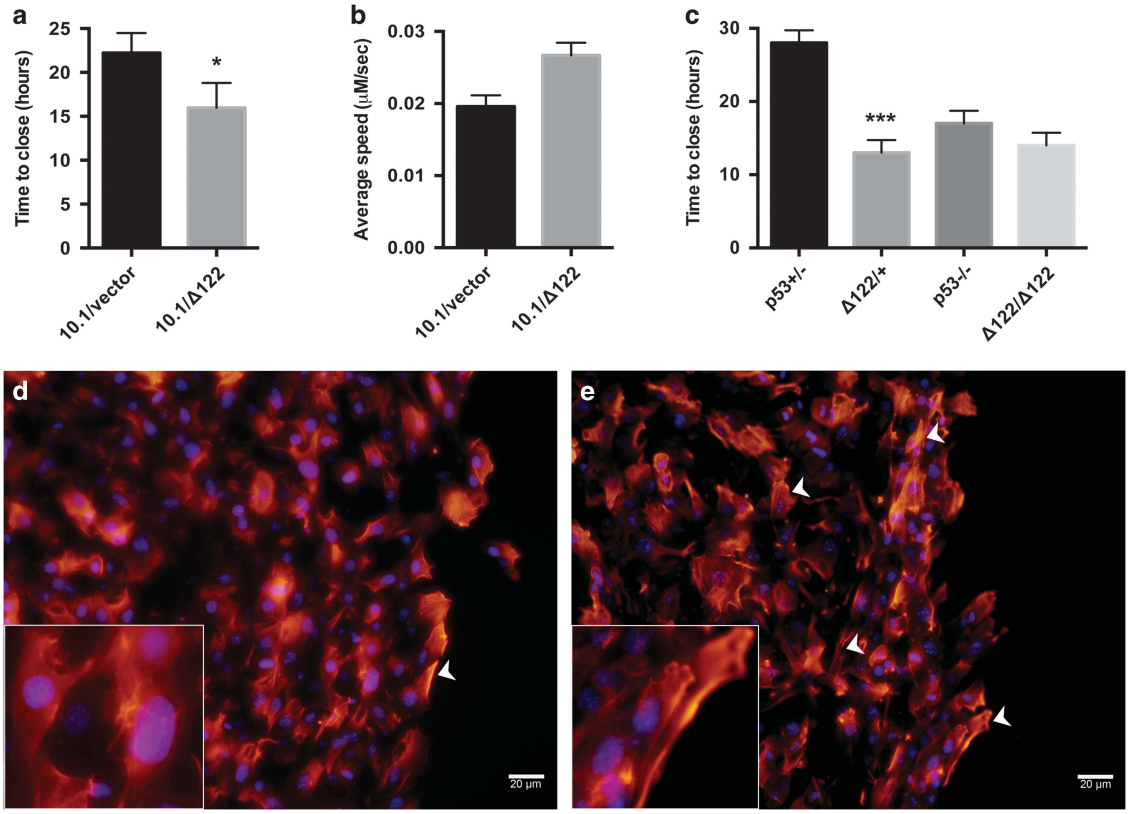

Figure 3. Expression of Δ122p53 promotes scratch wound closure. 10.1/vector, 10.1/Δ122, p53+/−, p53−/−, Δ122/+ and Δ122/Δ122 cells were seeded into 96-well plates, a scratch introduced into the monolayer and closure followed by time-lapse microscopy. (**a**) Time taken for cells to complete scratch wound closure for 10.1 cells. (**b**) Individual cells were tracked over time and the average speed of migration was determined. (**c**) Examples of the average time taken for MEF cells of indicated genotypes to complete scratch wound closure. (**d**) Immunofluorescence staining of 10.1/vector cells stained with phallodin (red) to label actin filaments and Hoechst (blue) to label DNA. Arrow heads indicate cells of interest. (**e**) Immunofluorescence staining of 10.1/Δ122 cells stained with phallodin (red) to label actin filaments and Hoechst (blue) to label DNA. Arrow heads indicate cells of interest.

and compared in Transwell assays with MEFs derived from Δ122p53/+/IL-6 knockout mice (Δ122p53/+/IL-6−/− cells). Results show that the loss of IL-6 reduces the number of migratory cells to one third of that on an IL-6 wt background (Figure 7d).

DISCUSSION

A preliminary analysis of Δ122p53 mice suggested that the Δ122p53 allele promotes tumour metastasis, as 10/14 mice expressing Δ122p53 showed evidence of metastatic sarcomas, something we have not seen in p53-null mice. To investigate how this occurs, we carried out a series of *in vitro* experiments using scratch wound and Transwell assays. We show that p53-null fibroblasts transduced with a Δ122p53 retrovirus had shortened scratch wound closure times and increased migration in a Transwell assay, as well as increased speed of migration. Consistent with this migratory phenotype, phalloidin staining of filamentous actin confirmed the migratory phenotype of cells expressing Δ122p53 and Δ133p53, with extensive elongation of filaments towards the leading edge observed compared with vector control cells at the earliest stages of scratch wound closure.

Experiments were also carried out with the human p53-null osteosarcoma cell line, Saos-2, that had been transduced with a retrovirus expressing the human Δ133p53 isoform. Results showed that Δ122p53 and Δ133p53 behave in a qualitatively similar manner in all experiments. We next extended these *in vitro* experiments using 3-dimensional organotypic assays using pancreatic cancer cells transduced with Δ122p53. Our results show that Δ122p53 increased the proportion of cells able to invade through the collagen matrix, with some evidence that Δ122p53 might also remodel the extracellular matrix, a process commonly seen in invasive and metastatic tumours. 'In addition, mice receiving B16 melanoma cells transduced with Δ122p53 developed lung metastases earlier than mice receiving B16/vector cells, and had larger and more invasive tumour colonies'. Thus, Δ122p53 can directly promote invasion *in vitro* and *in vivo*, and promote early development of metastatic tumours. These data support findings that inhibiting expression of Δ133p53 reduces the invasive ability of U87 glioblastoma cells.[17] Finally, using *in vitro* experiments, we show that Δ122p53 migration was dependent on soluble factors, notably IL-6 and CCL2, as migration was blocked with neutralizing antibodies to these factors, but not to other soluble factors we tested. Although Δ122p53 alone can increase the levels of these pro-migratory factors as evidenced by both scratch wound closure and Transwell assays with the various transduced cell lines, it is notable that when MEFs were used, heterozygous Δ122p53/+ MEFS were consistently more potent at promoting migration. This suggests that wt p53 is cooperating in some way to increase the levels of the relevant factors. In this context, we recently showed that Δ122p53 could cooperate with p53 to enhance its ability to induce cell cycle arrest after irradiation.[19] As such, it seems plausible that Δ122p53 might form heterodimers with wt (FL) p53 as shown for Δ40p53,[18] and in this manner stabilize a transcription complex on different promoters. In the case of the *IL-6* promoter, Δ122p53 would at the same time overcome the repression of this promoter by wt p53.[31] However, when Δ122p53 is at a higher concentration, as in

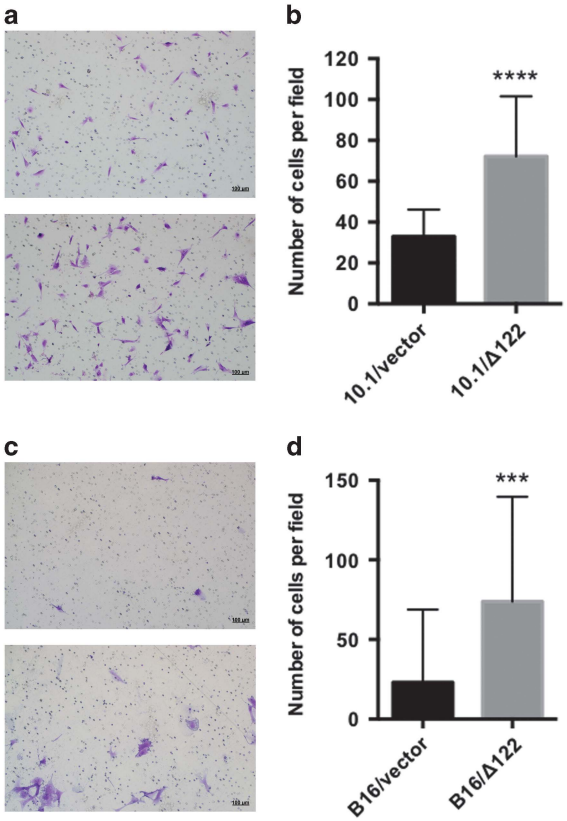

Figure 4. Overexpression of Δ122p53 promotes migration. 10.1/vector, 10.1/Δ122, B16/vector and B16/Δ122 cells were seeded into Transwell inserts as described previously and migrated cells stained with crystal violet. (**a**) Representative images of migrated 10.1/vector and 10.1/Δ122 cells after 4 h. (**b**) Quantitation of images comparing 10.1/vector and 10.1/Δ122. (**c**) Representative images of migrated B16/vector and B16/Δ122 cells after 72 h. (**d**) Quantitation of images comparing B16/vector and B16/Δ122 cells.

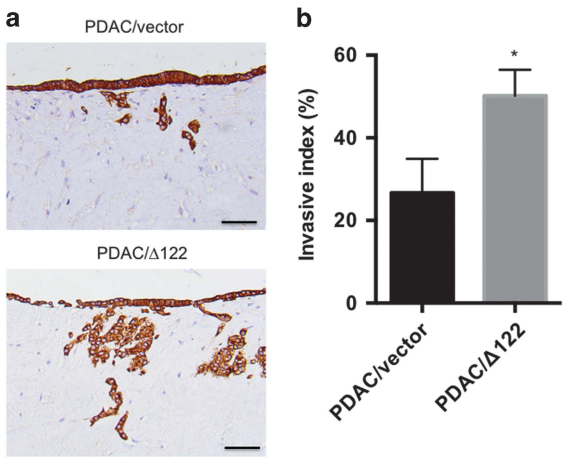

Figure 5. Δ122p53 promotes invasion in an organotypic model. (**a**) Pancytokeratin-stained sections of PDAC/vector (top) and PDAC/Δ122 (bottom) cells invading through collagen matrix contracted by telomerase-immortalised fibroblasts. Scale bar = 100 μm. (**b**) Quantitation of invasive index calculated as the percentage of PDACs invading relative to PDACs present in the layer overlaying the matrix.

the transduced cell lines, it may have sufficient DNA-binding ability to function alone to transactivate some genes. Indeed, we do find elevated levels of *IL-6* and *CCL2* transcripts in the Δ122p53-transduced cell lines (data not shown).

As outlined above, Δ133p53 is elevated in a number of human cancers,[11–15,32,33] and in some cases, this is associated with poor patient outcome.[16] This suggests that overexpression of Δ133p53 is associated with and may drive cancer progression. Our data showing that Δ122p53 and Δ133p53 promote a migratory phenotype *in vitro* and *in vivo* is consistent with this interpretation and with the observations that Δ133p53 can promote angiogenesis of glioblastoma cells.[17] These features are very reminiscent of the common gain-of-function tumour-associated p53 mutants, R175H and R273H,[22] which implies that Δ133p53 can in some circumstances function as a classical oncogene, such as when chronically overexpressed (as in the Δ122p53 mouse). Furthermore, if the cancer progression is mediated by soluble factors, such as CCL2 and IL-6 as our data suggest, tumours overexpressing Δ133p53 may be amenable to treatment by targeting these factors.

However, as Δ122p53 (and Δ133p53) can promote migration of both neoplastic and non-neoplastic cells, this suggests that the 'normal' function of Δ133p53 could be to activate a number of biological processes that involve migration, such as the chemotactic response of cells to infection and inflammation, in immune cell recruitment and in wound healing.

MATERIALS AND METHODS

Cells

Cell used in this study included MEFs derived from p53+/−, p53−/−, Δ122p53/+, Δ122p53/Δ122p53 and Δ122/+ IL-6 null animals, and stably transduced Saos-2 human osteosarcoma cells, 10.1 mouse fibroblasts and B16F1 melanoma cell lines. Saos-2 cells were obtained from Cell Bank Australia, 10.1 fibroblasts from Professor Wolfgang Deppert, Heinrich-Pette-Institut, Hamburg, Germany and B16F1 cells from Professor Michael Berridge, Malaghan Institute, Wellington, New Zealand. All cell lines were maintained in Dulbecco's modified Eagle medium (Gibco, Waltham, MA, USA) supplemented with 10% fetal calf serum (Moregate BioTech, Bulimba, QLD, Australia) in a humidified incubator at 5% CO_2 and 37 °C.

Animals

Δ122p53/Δ122p53 and Δ122p53/p53+ mice were aged and culled when tumour burden became apparent or when they lost 20% of original body weight, whichever was earlier. Animals (female C57BL/6, aged between 8 and 12 weeks) receiving transduced B16 cells intravenously were monitored twice daily for behaviour and weight alterations. Mice were culled when loss of normal behaviour was observed, or on day 18 post tumour cell injection, as a maximum end point. The group size of five animals per group was calculated to allow for detection of a 20% difference between mean colony number, assuming a standard deviation of 15. All animal research was granted institutional ethical approval by the University of Otago Animal Ethics Committee (AEC 3/12 and 35/15).

Histological analysis

Tissues were fixed in 10% neutral buffered formalin for 48 h and then transferred to 70% ethanol prior to paraffin embedding for histological analysis to identify tumour type on the basis of cellular morphology. Sections were then cut at 4 μm, mounted on DakoFlex slides (Dako, Glostrup, Denmark), and stained with haematoxylin and eosin. Organs selected for the study included brain, heart, gut, salivary glands, lung, spleen, liver, kidney, thymus, pancreas, lymph nodes and occasional bone specimens. Slides were scanned using the Aperio ScanScope CS digital imaging system (Leica Biosystems, Wetzlar, Germany). Tumour area was determined by serially sectioning through the lungs and using ImageJ to measure the area of the tumour in each section. The data showing metastasis in multiple organs are a representative example of that found in 10 animals. Tumour area was measured on one animal of each genotype, with blinding to the assigned group, while tumour colony and histology examples shown are representative of that found in five animals.

Construction of transduced lines

To produce stable cell lines expressing Δ133p53 or Δ122p53, amphotrophic replication deficient Phoenix cells were transfected with vectors carrying Δ133p53, Δ122p53 or a matched empty control vector. Media

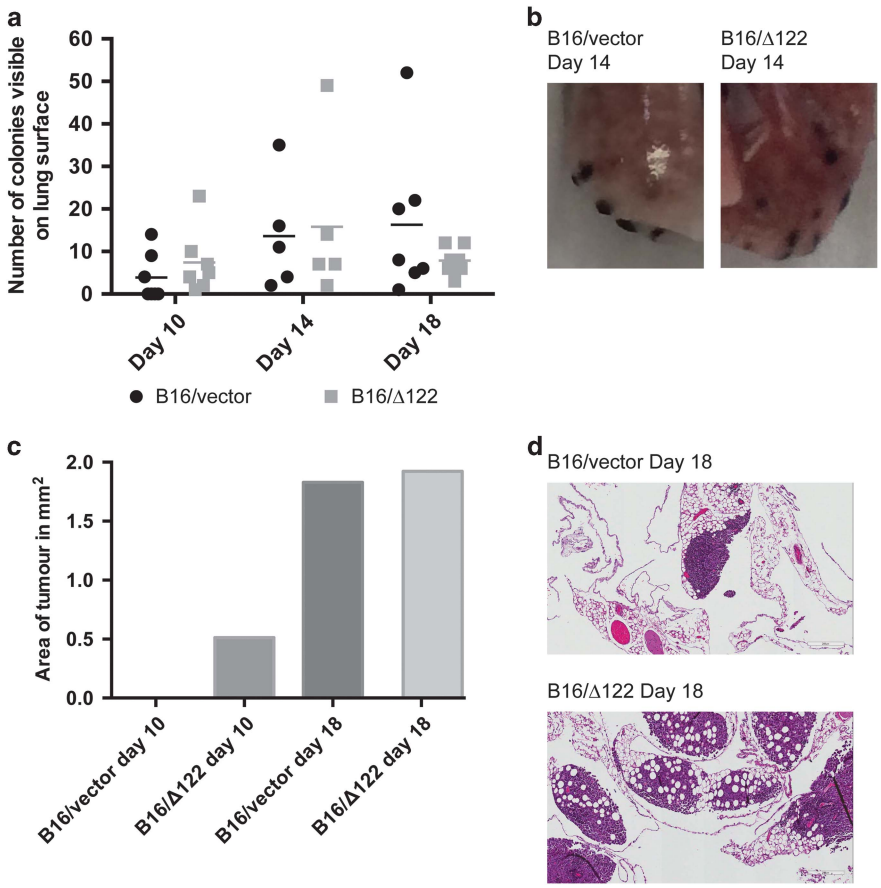

Figure 6. Δ122p53 promotes invasion and metastasis of B16F1 melanoma. B16/vector and B16/Δ122 cells were injected intravenously into mice and animals culled at days 10, 14 and 18. (**a**) Number of tumour colonies counted on the lung surface at each time point. (**b**) Representative examples of lung colonies counted at day 14. (**c**) Histological quantitation of area of tumours in serially sectioned lungs. (**d**) Representative images showing the extent of lymphocytic infiltration and tumour cell invasion into associated adipose tissue of tumour-bearing lungs.

from transfected cells was then applied to Saos-2, 10.1, PDAC and B16F1 target cell lines for three transfers. Five cell passages of target cells ensured stable transduction. Cells were then sorted on GFP expression to ensure a homogenous transduced population.

Generation of CM

p53+/−, p53−/−, Δ122p53/+ and Δ122p53/Δ122p53 MEFs were grown under normal cell culture conditions for 3–4 days or until approximately 70–80% confluent. Conditioned media was then collected from cells and used for scratch wound assays.

Scratch wound assays

Cells were seeded into 96-well Essen Bioscience (Ann Arbor, MI, USA) ImageLock plates and grown to confluence. Scratch wounds were introduced into the cell monolayer using the Essen 96-pin WoundMaker. Media was aspirated from the wells and cells were rinsed twice in phosphate-buffered saline to remove all non-adherent cells before replacement of media. Cells were then monitored over time at 2–3 h intervals using the IncuCyte FLR and accompanying software. Time to closure was taken as the time when wound width reached 0 μm. Saos-2 time to closure is a representative example of three biological replicates with 24 technical replicates. 10.1 time to closure shows three biological replicates. p53 MEF time to closure is a representative example of four biological replicates with three technical replicates shown. p53+/− MEF with CM shows two biological replicates.

Single cell tracking experiments

Saos-2 and 10.1 transduced cells were seeded into glass-bottomed 35-mm diameter dishes and allowed to reach confluency. Once 100% confluent, scratch wounds were introduced using a p200 tip, cells washed three times with phosphate-buffered saline and media replaced. Cells were then monitored using the Cell Voyager live imaging microscope (Yokogawa, Japan) and images taken every 5 min for 16–48 h. Saos-2 speed and persistence represents three biological replicates. 10.1 speed represents two biological replicates.

Transwell assays

Cells were serum-starved in medium with 0.5% fetal calf serum for 24 h while sub-confluent, then harvested, resuspended in serum-deficient medium, and seeded into 8-μm Transwell inserts. After 4–72 h depending on the cell line, cells were fixed, stained, imaged and analysed using ImageJ. Transduced Saos-2 cells were seeded as described, with the addition of an overlay of Matrigel on the Transwell membrane. Transwell images were taken with blinding to the genotypes of the cells to ensure no bias was introduced. Saos-2 migration represents two biological replicates, shown as four technical replicates. 10.1 and B16 migration shows 10 and 4 biological replicates, respectively. IL-6 blocking represents five biological replicates. CCL2 blocking represents four biological replicates, presented as six technical replicates. IL-6 null MEFs represents three biological replicates.

Staining of actin filaments with phalloidin

Cells were seeded into 24-well plates and a scratch wound introduced using a p200 tip when the cells were confluent. Cells were allowed to migrate to close the scratch wound for 2 h, then fixed in 2% paraformaldehyde in phosphate-buffered saline, blocked and permeabilised in 5% bovine serum albumin/0.2% Triton, then stained with phallodin-568 (A12380; Alexa Fluor; 1:500; Molecular Probes, Waltham, MA, USA) to label the actin filaments and Hoechst 33342 (H1399; 1:1000; Molecular Probes) to label the DNA. Cells were then imaged with an Olympus (Tokyo, Japan) IX71 inverted microscope at ×200 and images merged using Adobe Photoshop CS3. Both Saos-2 and 10.1 cell labelling are representative examples of two and four technical replicates, respectively.

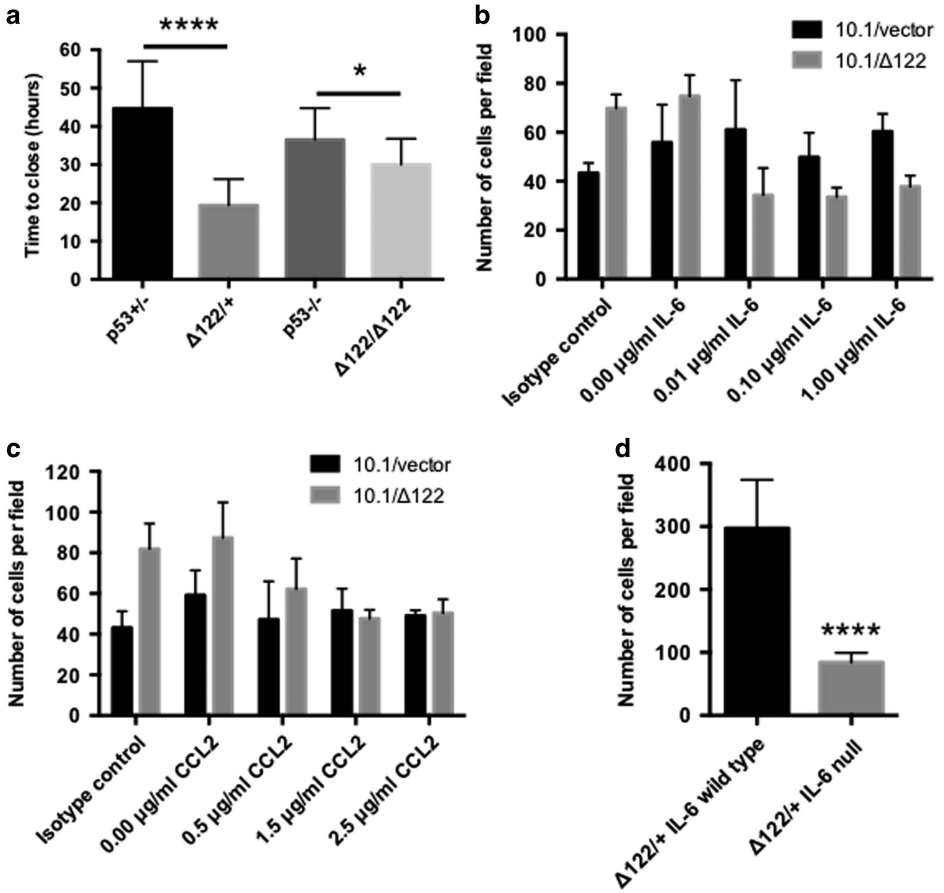

Figure 7. Cell migration promoted by Δ122p53 requires the cytokine IL-6. (**a**) p53+/− MEFs were seeded in CM that had been derived from MEFs of the indicated genotypes. A scratch was introduced into the confluent monolayer and the times to closure were determined. (**b**) Serum-starved 10.1/vector and 10.1/Δ122 cells were used in a Transwell assay with the addition of a blocking antibody to IL-6. (**c**) Serum-starved 10.1/vector and 10.1/Δ122 cells were used in a Transwell assay with the addition of a blocking antibody to CCL2. (**d**) Δ122p53/+ MEFs and MEFs derived from isogenic Δ122p53/+/IL-6−/− mice were seeded as above into Transwell inserts and the number of cells that had migrated after 4 h determined.

Proliferation assays with amsacrine

10.1/vector and 10.1/Δ122 cells were seeded into 96-well plates, dosed with a range of concentrations of amsacrine and proliferation monitored over time using the IncuCyte FLR and accompanying software. Once an appropriate concentration was established, at which growth was prevented but toxicity was minimal, a scratch wound assay was performed with the addition of amsacrine when the media was replaced after the wound was made.

Organotypic invasion assay

Invasion of PDAC cells through collagen I matrices contracted by either telomerase-immortalised fibroblasts, p53+/+ or Δ122p53/+ MEFs were performed as previously described.[24] Briefly, quiescent fibroblasts were embedded into a collagen I solution (8×10^4 cells/matrix). Polymerised matrices were then allowed to contract over 12 days in complete media (Dulbecco's modified Eagle medium, supplemented with 10% fetal calf serum) and renewed at day 6 of contraction. When the matrices were contracted, 4×10^4 PDAC cells were seeded on top of the matrix and grown for 4–5 days until confluent. The matrices were then transferred to a liquid–air grid interface and left to invade for 12 days. Samples were then fixed in 10% neutral buffered formalin for 24 h and embedded in paraffin for histological analyses. Data shown are from three biological replicates.

Histological analysis of organotypic invasion assay

Histological staining was performed on 4-μm sections deparaffinised in xylene and rehydrated using graded ethanol washes. Immunohistochemistry staining for pancytokeratin was performed used the Leica Bond RX system (1:50; C-11; Leica-Novocastra, Nußloch, Germany). For scoring of the invasive index, three images per sample were acquired using a bright field microscope (Leica DM4000). Invasive index = (invasive cells)/(non invading cells+invasive cells).

Bio-Plex

To screen for candidate factors responsible for the increased migration, CM from 10.1/vector and 10.1/Δ122 cells were analysed for expression of a number of cytokines using a Bio-Plex Pro Mouse Cytokine 23-plex Assay (Bio-Rad, Hercules, CA, USA). Data shown are from two biological replicates.

Statistical analyses

All raw data were analysed in Prism 6 (GraphPad Software) for statistical analysis. All data are presented as the mean ± 1s.d., except for the Saos-2 migration speed and persistence, 10.1 migration speed experiments and organotypic invasion assays, which are presented as the mean ± s.e.m. Statistical differences between two groups were evaluated using an unpaired t test, with a P value of <0.05 taken as a significant difference (* <0.05, ** <0.01, *** <0.001, **** <0.0001).

ABBREVIATIONS

FBS, foetal bovine serum; FL, full-length; IL-6, interleukin-6; MEF, mouse embryonic fibroblast; PDAC, pancreatic ductal adenocarcinoma; TP53, human p53 gene; WT, wild type

CONFLICT OF INTEREST

The authors declare no conflict of interest.

ACKNOWLEDGEMENTS

This work was supported by the Health Research Council of New Zealand, Marsden Fund, Maurice Wilkins Centre for Molecular Biodiscovery, Cancer Council NSW and National Health and Medical Research Council.

REFERENCES

1 Alexandrova A, Ivanov A, Chumakov P, Kopnin B, Vasiliev J. Changes in p53 expression in mouse fibroblasts can modify motility and extracellular matrix organization. *Oncogene* 2000; **19**: 5826–5830.
2 Gadea G, Lapasset L, Gauthier-Rouviere C, Roux P. Regulation of Cdc42-mediated morphological effects: a novel function for p53. *EMBO J* 2002; **21**: 2373–2382.
3 Guo F, Gao Y, Wang L, Zheng Y. p19Arf-p53 tumor suppressor pathway regulates cell motility by suppression of phosphoinositide 3-kinase and Rac1 GTPase activities. *J Biol Chem* 2003; **278**: 14414–14419.
4 Guo F, Zheng Y. Rho family GTPases cooperate with p53 deletion to promote primary mouse embryonic fibroblast cell invasion. *Oncogene* 2004; **23**: 5577–5585.
5 Gadea G, de Toledo M, Anguille C, Roux P. Loss of p53 promotes RhoA-ROCK-dependent cell migration and invasion in 3D matrices. *J Cell Biol* 2007; **178**: 23–30.
6 Ravi R, Mookerjee B, Bhujwalla ZM, Sutter CH, Artemov D, Zeng Q *et al.* Regulation of tumor angiogenesis by p53-induced degradation of hypoxia-inducible factor 1alpha. *Genes Dev* 2000; **14**: 34–44.
7 Rastinejad F, Polverini PJ, Bouck NP. Regulation of the activity of a new inhibitor of angiogenesis by a cancer suppressor gene. *Cell* 1989; **56**: 345–355.
8 Good DJ, Polverini PJ, Rastinejad F, Le Beau MM, Lemons RS, Frazier WA *et al.* A tumor suppressor-dependent inhibitor of angiogenesis is immunologically and functionally indistinguishable from a fragment of thrombospondin. *Proc Natl Acad Sci USA* 1990; **87**: 6624–6628.
9 Marcel V, Dichtel-Danjoy ML, Sagne C, Hafsi H, Ma D, Ortiz-Cuaran S *et al.* Biological functions of p53 isoforms through evolution: lessons from animal and cellular models. *Cell Death Differ* 2011; **18**: 1815–1824.
10 Senturk S, Yao Z, Camiolo M, Stiles B, Rathod T, Walsh AM *et al.* p53Psi is a transcriptionally inactive p53 isoform able to reprogram cells toward a metastatic-like state. *Proc Natl Acad Sci USA* 2014; **111**: E3287–E3296.
11 Bourdon JC, Fernandes K, Murray-Zmijewski F, Liu G, Diot A, Xirodimas DP *et al.* p53 isoforms can regulate p53 transcriptional activity. *Genes Dev* 2005; **19**: 2122–2137.
12 Boldrup L, Bourdon JC, Coates PJ, Sjostrom B, Nylander K. Expression of p53 isoforms in squamous cell carcinoma of the head and neck. *Eur J Cancer* 2007; **43**: 617–623.
13 Avery-Kiejda KA, Zhang XD, Adams LJ, Scott RJ, Vojtesek B, Lane DP *et al.* Small molecular weight variants of p53 are expressed in human melanoma cells and are induced by the DNA-damaging agent cisplatin. *Clin Cancer Res* 2008; **14**: 1659–1668.
14 Song W, Huo SW, Lu JJ, Liu Z, Fang XL, Jin XB *et al.* Expression of p53 isoforms in renal cell carcinoma. *Chinese Med J* 2009; **122**: 921–926.
15 Fujita K, Mondal AM, Horikawa I, Nguyen GH, Kumamoto K, Sohn JJ *et al.* p53 isoforms Delta133p53 and p53beta are endogenous regulators of replicative cellular senescence. *Nat Cell Biol* 2009; **11**: 1135–1142.
16 Nutthasirikul N, Limpaiboon T, Leelayuwat C, Patrakitkomjorn S, Jearanaikoon P. Ratio disruption of the 133p53 and TAp53 isoform equilibrium correlates with poor clinical outcome in intrahepatic cholangiocarcinoma. *Int J Oncol* 2013; **42**: 1181–1188.
17 Bernard H, Garmy-Susini B, Ainaoui N, Van Den Berghe L, Peurichard A, Javerzat S *et al.* The p53 isoform, Delta133p53alpha, stimulates angiogenesis and tumour progression. *Oncogene* 2013; **32**: 2150–2160.
18 Hafsi H, Santos-Silva D, Courtois-Cox S, Hainaut P. Effects of Delta40p53, an isoform of p53 lacking the N-terminus, on transactivation capacity of the tumor suppressor protein p53. *BMC Cancer* 2013; **13**: 134.
19 Slatter TL, Hung N, Bowie S, Campbell H, Rubio C, Speidel D *et al.* Delta122p53, a mouse model of Delta133p53alpha, enhances the tumor-suppressor activities of an attenuated p53 mutant. *Cell Death Dis* 2015; **6**: e1783.
20 Slatter TL, Hung N, Campbell H, Rubio C, Mehta R, Renshaw P *et al.* Hyperproliferation, cancer, and inflammation in mice expressing a Delta133p53-like isoform. *Blood* 2011; **117**: 5166–5177.
21 Muller PA, Caswell PT, Doyle B, Iwanicki MP, Tan EH, Karim S *et al.* Mutant p53 drives invasion by promoting integrin recycling. *Cell* 2009; **139**: 1327–1341.
22 Muller PA, Vousden KH, Norman JC. p53 and its mutants in tumor cell migration and invasion. *J Cell Biol* 2011; **192**: 209–218.
23 Johnson RK, Wodinsky I, Swiniarski J, Meaney KF, Clement JJ. Interaction of gamma-irradiation with two new antineoplastic agents, aziridinylbenzoquinone (AZQ) and 4'-(acridinylamino)methanesulfon-m-anisidide (AMSA), in murine tumors in vivo. *Int J Radiat Oncol Biol Phys* 1979; **5**: 1605–1609.
24 Timpson P, McGhee EJ, Erami Z, Nobis M, Quinn JA, Edward M *et al.* Organotypic collagen I assay: a malleable platform to assess cell behaviour in a 3-dimensional context. *J Vis Exp* 2011; (56): e3089.
25 Fidler IJ. Selection of successive tumour lines for metastasis. *Nat New Biol* 1973; **242**: 148–149.
26 Coppe JP, Patil CK, Rodier F, Sun Y, Munoz DP, Goldstein J *et al.* Senescence-associated secretory phenotypes reveal cell-nonautonomous functions of oncogenic RAS and the p53 tumor suppressor. *PLoS Biol* 2008; **6**: 2853–2868.
27 Carr MW, Roth SJ, Luther E, Rose SS, Springer TA. Monocyte chemoattractant protein 1 acts as a T-lymphocyte chemoattractant. *Proc Natl Acad Sci USA* 1994; **91**: 3652–3656.
28 Davatelis G, Tekamp-Olson P, Wolpe SD, Hermsen K, Luedke C, Gallegos C *et al.* Cloning and characterization of a cDNA for murine macrophage inflammatory protein (MIP), a novel monokine with inflammatory and chemokinetic properties. *J Exp Med* 1988; **167**: 1939–1944.
29 Bystry RS, Aluvihare V, Welch KA, Kallikourdis M, Betz AG. B cells and professional APCs recruit regulatory T cells via CCL4. *Nat Immunol* 2001; **2**: 1126–1132.
30 Blay JY, Negrier S, Combaret V, Attali S, Goillot E, Merrouche Y *et al.* Serum level of interleukin 6 as a prognosis factor in metastatic renal cell carcinoma. *Cancer Res* 1992; **52**: 3317–3322.
31 Gudkov AV, Gurova KV, Komarova EA. Inflammation and p53: a tale of two stresses. *Genes Cancer* 2011; **2**: 503–516.
32 Anensen N, Oyan AM, Bourdon JC, Kalland KH, Bruserud O, Gjertsen BT. A distinct p53 protein isoform signature reflects the onset of induction chemotherapy for acute myeloid leukemia. *Clin Cancer Res* 2006; **12**: 3985–3992.
33 Hofstetter G, Berger A, Fiegl H, Slade N, Zoric A, Holzer B *et al.* Alternative splicing of p53 and p73: the novel p53 splice variant p53delta is an independent prognostic marker in ovarian cancer. *Oncogene* 2010; **29**: 1997–2004.

Supplementary Information accompanies this paper on the Oncogene website (http://www.nature.com/onc)